PROCEEDINGS OF SCIENCE

Goals, Development, and Performance of the Compton Spectrometer and Imager's Anti-Coincidence Subsystem

Parshad Patel,[a,*] **Lee Mitchell,**[b] **Eric Wulf,**[b] **Clio Sleator,**[b] **Anthony Hutcheson,**[b] **Andreas Zoglauer**[c] **and John Tomsick**[c]

[a] *George Mason University, 4400 University Dr, Fairfax, VA 22030, USA*

[b] *US Naval Research Laboratory, 4555 Overlook Ave SW, Washington, DC 20375, USA*

[c] *Space Sciences Laboratory, University of California, 7 Gauss Way, Berkeley, CA 94720, USA*

E-mail: parshadkp@gmail.com

The Compton Spectrometer and Imager (COSI) is an upcoming NASA Small Explorer mission focused on exploring the 0.2-5 MeV energy range in the electromagnetic spectrum. This MeV gap has long been underexplored due to technical challenges, in particular the high instrument and astrophysical backgrounds in this energy regime. COSI aims to conduct spectroscopy, imaging, and polarimetry of cosmic gamma-ray sources to study galactic positrons, galactic element formation, accreting black holes, and contribute to multi-messenger astrophysics. COSI utilizes sixteen germanium detectors (GeDs) for high-resolution spectroscopy and an Anti-Coincidence Subsystem (ACS) comprised of twenty-two Bismuth Germanate (BGO) scintillation crystals coupled with Silicon Photomultipliers (SiPMs). The ACS provides active shielding, detects γ-rays escaping the GeDs, monitors background radiation, and triggers transient alerts. Achieving a low energy threshold for the ACS is crucial for anti-coincidence vetoing and detecting transients. For COSI's ACS, SiPMs have been selected over photomultiplier tubes (PMTs) due to their low voltage, weight, and volume. Contrary to other scintillators which prefer a large number of SiPMs to read out the signal, we find that a 3×3 SiPM array centered on the narrow side of a BGO scintillator is enough to provide the best possible energy threshold. In this research, we provide an overview of the COSI ACS detector system, and report on results from various performance tests of the BGO detectors and the flight-like readout system.

39th International Cosmic Ray Conference (ICRC2025)
15–24 July 2025
Geneva, Switzerland

*Speaker

PoS(ICRC2025)799

1. Introduction

The Compton Spectrometer and Imager explores the low-energy γ-ray regime, which holds clues to key astrophysical questions, including: 1. the origin of the 511 keV antimatter annihilation γ-ray line coming from the Galactic Center region as first seen over 50 years ago by [1] 2. the life cycles of massive stars and their supernovae [2]; 3. polarization in extreme environments such as GRBs, black holes, and AGN [3]; and 4. multi-messenger astrophysics in the "MeV Gap".

COSI is composed of sixteen high spectral resolution GeDs that provide 3D positions of γ-ray interaction sites along with an Anti-Coincidence Subsystem (ACS) that shields the telescope on five sides. Compton telescopes like COSI detect γ-rays through multiple Compton scattering events which end in a final photo-absorption event in the instrument. The energy of the imparting γ-ray is determined by adding up the individual interaction energies and the the Compton angle measured from an axis defined by the first and second interactions defines an event circle on the sky ([4] and references therein). For a more complete overview of COSI, see [5].

The ACS consists of five walls that surround the GeDs on the sides and the bottom. The ACS functions as an excellent γ-ray and anti-coincidence monitor with two energy bands, low-energy, 80 keV to 2 MeV, and high-energy, starting at 2 MeV. This paper will focus on the development and the performance of the BGO detectors on the ACS.

Germanium Strip Detectors on COSI. COSI utilizes a compact array of cross-strip GeDs, enabling precise identification of individual γ-ray interactions with exceptional spectral and spatial resolution. The sixteen GeDs, arranged in a 4×4 array with detector size of $8 \times 8 \times 1.5$ cm^3, are housed in a cryostat and read out using custom Application-Specific Integrated Circuits (ASICs). Each GeD has 64 strip electrodes per side running in orthogonal directions on the two sides along with an additional guard ring (GR) electrode which acts as a veto signal. To simplify the readout system, the ACS uses the same type of NRL4 ASICs [6]) to read out the BGO crystals.

Bismuth Germanate Detectors on COSI's ACS. The four side ACS walls consists of three BGO crystals each with the bottom wall consisting of ten crystals. A model of the COSI ACS along with a cross section of the X-Wall is depicted in Fig. 1. The wall frame is made of aluminum to allow γ-rays enter the BGO scintillators. BGO is preferred to other scintillation crystals due to their high density, resulting in a very effective shielding for the GeDs from background γ-rays. Incident γ-rays interact with BGO crystals to produce visible light that can be correlated to the corresponding γ-ray. BGO crystal sizes in the ACS are shown in Tab. 1. These BGO detectors are used to veto events in the GeDs that are not in the field of view of the instrument.

	X [cm]	Y [cm]	Z [cm]
BGO X-Wall	19.4	11.8	2.30
BGO Y-Wall	19.4	11.0	2.30
BGO Z-Wall 1	19.8	6.25	2.40
BGO Z-Wall 2	17.1	6.45	2.40
BGO Z-Wall 3	19.8	8.05	2.40

Table 1: Dimensions of different sized BGO scintillation crystals. BGO scintillators have a tolerance of ± 0.2 mm in all three dimensions.

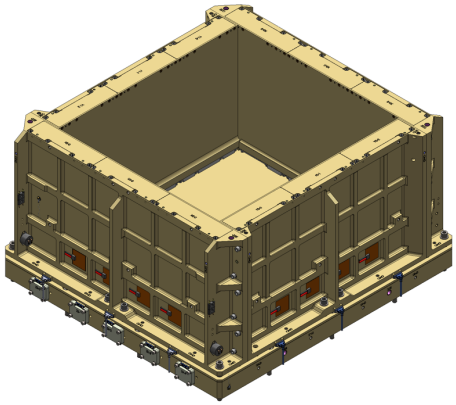

(a) Model of the assembled COSI's ACS walls.

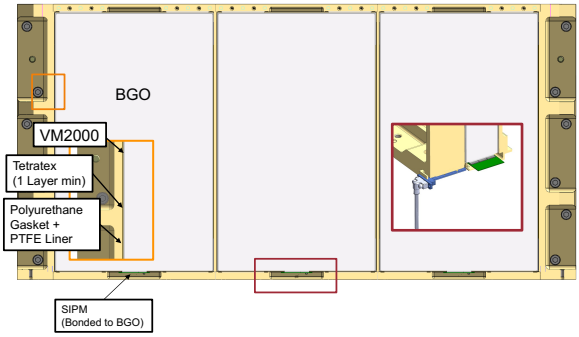

(b) Assembled BGO detectors enclosed in the X-Wall of the ACS housing. SiPM interface and wrapping layers on the BGO detectors and the X-Wall is also shown.

Figure 1: Compton Spectrometer and Imager's Anti-Coincidence Subsystem system.

Crystal	BGO	CsI	CsI:T1	CsI:Na	NaI:T1
Density [g/cm^3]	7.13	4.51	4.51	4.51	3.67
Hygroscopicity	No	Slight	Slight	Yes	Yes
Decay Time (ns)	300	30	1120	690	245
Light Yield[a]	21	3.6	165	88	100
Leading Atomic Number Z ($_Z$X)	$_{83}$Bi	$_{55}$Cs	$_{55}$Cs	$_{55}$Cs	$_{11}$Na

[a] Relative light output with QE of the readout device taken out for samples of 1.5 X0 with Tyvek wrapping.

Table 2: Scintillation crystal properties from [7].

2. Development and Performance of the BGO Detectors in the COSI ACS

Visible light from the BGO scintillators is detected by a passively summed array of Onsemi J-Series 6x6 mm SiPMs, optically coupled to the smallest face of each crystal using Dow Dowsil 93-500 Space Grade Encapsulant. To maximize light collection, the crystals are wrapped in reflective material. The SiPMs convert the scintillation light to current, which is read out using NIM shaping amplifier and a Amptek Multi-Channel Analyzer (MCA) or the NRL4 ASIC. All data in this paper were collected with an MCA and amplifier, except for Sec. 2.5, which used an Engineering Model (EM) Shield Control Board.

BGO is preferred over other scintillators for its high density and non-hygroscopic nature (Tab. 2). Achieving equivalent shielding with Cesium Iodide (CsI) or Sodium Iodide (NaI) would require crystals 1.3 cm and 2.2 cm thicker, respectively, along the Z-axis compared to the COSI Flight Model (FM) X-Wall BGO. While BGO's ruggedness makes it ideal for shielding and background monitoring, its low light yield leads to some unexpected behavior. Unlike most scintillators, where performance improves with more SiPMs, reading out BGO on the smallest edge performs best with a 3×3 SiPM array, balancing electronic noise and signal. The following sections detail improvements to BGO detector performance, with spectra fit using a Gaussian emission line plus a linear background.

Energy threshold [keV]	Relative photon flux [b] (larger is better)	Relative COSI sensitivity @ 511 keV [%] (smaller is better)
50	1	99
80	0.86	100
100	0.79	101
150	0.64	104
200	0.53	-
300	0.37	-
∞	-	220

[b] integrated from energy threshold [keV] to 1 MeV

Table 3: Dependence of parameters key to ACS performance on energy threshold. The short GRB photon flux is modeled using a Band function with parameters from [8]: $\alpha = -0.5$, $\beta = -2.3$, and $E_{\text{break}} = 490$ keV. Relative COSI sensitivity to the positron annihilation line (511 keV), enabled by ACS background rejection, is also presented at various ACS energy thresholds.

2.1 Primary Requirements of the ACS

The primary requirement of the ACS is a low energy threshold, essential for vetoing low-energy gamma-rays scattering in or out of the GeDs. Relative COSI sensitivity to the positron annihilation line (511 keV) for different energies is shown in Tab. 3. A low energy threshold for the ACS is necessary to detect events that escape the GeDs without depositing their full energy, and the COSI sensitivity degrades as the ACS energy threshold increases. With the large effective area of the ACS, larger than the Fermi-LAT, the ACS is a great GRB monitor. Tab. 3 shows that the COSI sensitivity and the relative photon flux is worse with increasing energy thresholds, especially after reaching 100-150 keV. Energy resolution of the BGO detectors is less of a concern, since the reported energy bins are large. Hence, the tests below will focus less on the energy resolution and more on the energy threshold of the BGO detectors.

2.2 Wrapping of BGO Detectors

We began by studying the BGO response to various types of wrapping techniques. These BGO scintillators are wrapped with 3 types of reflective wrapping. Through testing, we found that the optimal wrap for our crystals is 2 layers of VM2000 (thin, 65 μm non-metallic specular reflector used by [9] on the Fermi-LAT calorimeter), 1 layer of PTFE Tetratex (white teflon based wrap that forms around the VM2000), and one layer of PTFE Teflon (76 μm). Furthermore, we compared the performance of the BGO detectors with VM2000 that is either heat molded or scored using a 3 1/2" PMT on the small face of the crystal. The crystal was tested in a black box for light tightness.

From Fig. 2 we see that molded VM2000 performs better than scored VM2000 with a lower energy threshold and energy resolution that is improved from from 11.7% (scored) to 10.76% (molded) at 662 keV. For the COSI FM crystals, the wrapping was modified to include additional PTFE Teflon layer on top of the PTFE Tetratex and it merely aids in the assembly of these detectors into the ACS housing. A COSI ACS EM X-Wall detector wrapped with two layers of VM2000, one layer of PTFE Tetratex, and one layer of PTFE Teflon is pictured in Fig. 5.

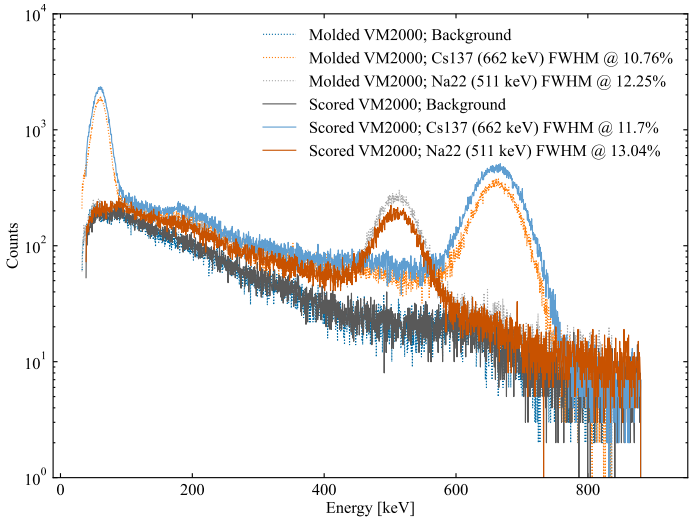

Figure 2: Comparisons of energy resolutions at 511 keV and 662 keV of different wrapping methods. These methods include 2 Layers of VM2000, 1 layer of PTFE Tetratex. Tested with a 3-1/2" PMT with a 800V Bias. Data calibrated using peaks from ^{241}Am (60 keV), ^{22}Na (511 keV), and ^{137}Cs (662 keV).

2.3 Optimal Number of SiPMs for COSI's BGO Detectors

After determining the optimal BGO wrapping method, we optimized the number of SiPMs. SiPMs are pixelated photodetectors that convert visible light into current and are combined into arrays to sum their signals. The arrays used in these tests are shown in Fig. 3b and 3c. The 16×1 array includes 0Ω resistors that can be removed to disable individual SiPMs.

The SiPM boards are optically coupled to the smallest face of the BGO crystal using optical pads. Unlike other scintillators that benefit from full-face SiPM coverage, BGO achieves comparable or better energy thresholds with fewer SiPMs, as shown in Fig. 3a, due to its low light output. Hence, a 3×3 SiPM array was chosen for the ACS FM BGO detectors because it consumes less power than larger arrays and offers the best signal-to-noise balance, yielding a low energy threshold.

We also tested the optimal SiPM placement by comparing centered and off-centered 2×2 SiPM arrays (not pictured) optically coupled to the COSI EM BGO crystal. As shown in Fig. 4a and configurations in Fig. 4c and 4b, the centered array yields slightly better energy threshold and resolution at 662keV. The ^{241}Am (60keV) peak is also more distinct in the centered case, supporting the choice to center the 3×3 SiPM arrays in the COSI FM BGO detectors.

2.4 Uniformity Testing on COSI's BGO Detectors

Since γ-rays can interact with the BGO detectors from all directions, the first step before the FM build is to verify detector uniformity. We perform a 12-point scan using a ^{137}Cs source (Fig. 6a), with outer points placed 10 cm from the crystal edge and the others spaced evenly across each row. As shown in Fig. 6, the position nearest the SiPM yields the best performance, while the remaining points show comparable energy resolution at 662 keV.

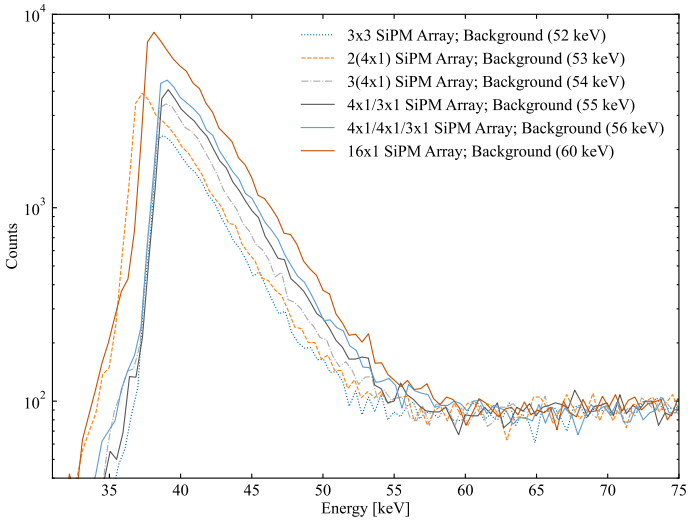

(a) Calibrated dataset shown for different SiPM arrays with energy thresholds noted in the legend inside parenthesis. Other SiPM configurations with the 1×16 SiPM board (not plotted) were also tested but resulted in a worse energy threshold. Data calibrated using peaks from ^{241}Am (60 keV), ^{22}Na (511 keV), and ^{137}Cs (662 keV).

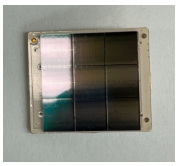

(b) 3×3 SiPM array board.

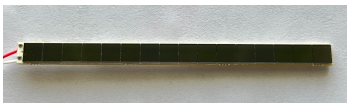

(c) 1×16 SiPM with 0 Ω resistors to activate or deactivate SiPMs.

Figure 3: Energy threshold comparison between various SiPM arrays (Fig. 3a). The 3×3 SiPM board (Fig. 3b) and the 1×16 SiPM board (Fig. 3c) with configurations of 2(4×1), 3(4×1), 4×1/3×1, and 4×1/4×1/3×1.

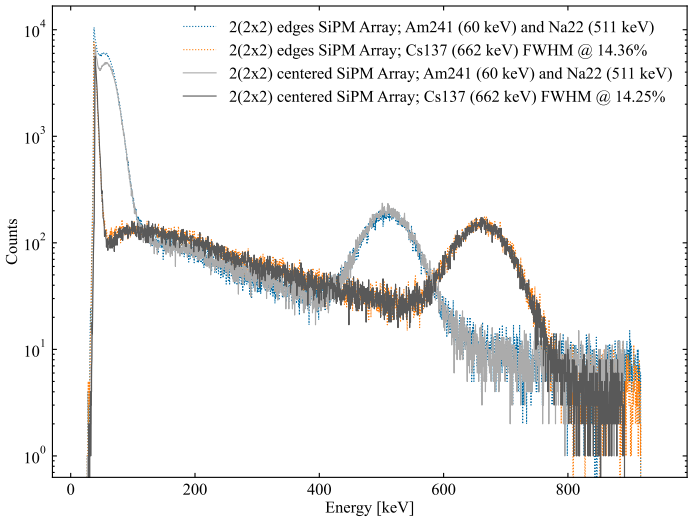

(a) SiPM array comparison for energy thresholds and resolution for two 2×2 arrays centered and not centered on the small face of COSI EM BGO crystal. Edge case measured an energy threshold of 59 keV and center case measured an energy threshold of 54 keV. Data calibrated using peaks from ^{241}Am (60 keV), ^{22}Na (511 keV), and ^{137}Cs (662 keV).

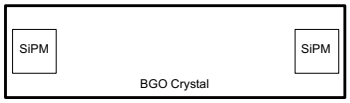

(b) Edge configuration for the SiPM comparison test for positional dependence.

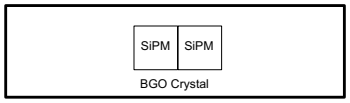

(c) Center configuration for the SiPM comparison test for positional dependence.

Figure 4: Positional dependence of the SiPMs on to the face of the BGO crystal. Plots show the calibrated spectra and the configuration of the SiPMs with respect to the face of the BGO crystal.

Figure 5: A fully wrapped BGO detector used for the EM X-Wall ACS System as pictured in Fig. 1b.

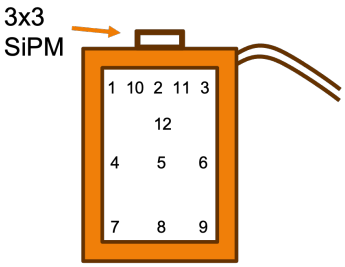

(a) Source position map for uniformity testing.

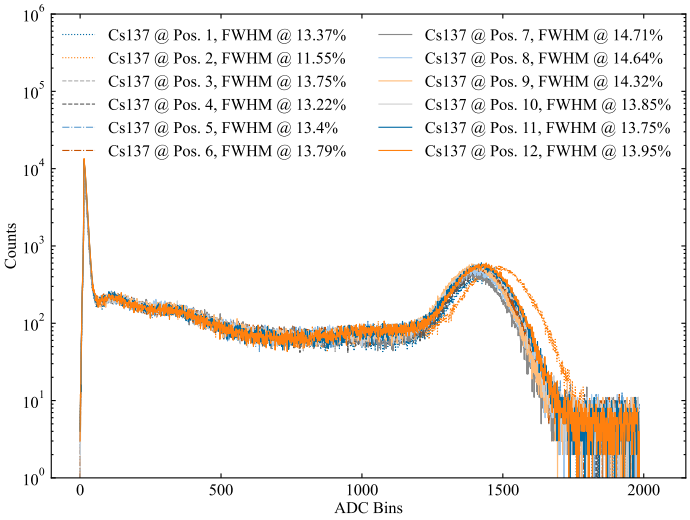

(b) Uncalibrated spectra of a collimated scan using a ^{137}Cs source placed at numerous positions as shown in Fig. 6a. Energy resolution for ^{137}Cs (662 keV) obtained from data calibrated using peaks from ^{241}Am (60 keV), ^{22}Na (511 keV) and ^{137}Cs (662 keV). A collimated scan at Pos. 2 (dotted orange line) results in a peak that has a higher gain than the rest.

Figure 6: Collimated source testing of the BGO detectors done after vibrational and thermal testing to characterize the uniformity of BGO detectors. Data shown for EM BGO detector 2.

2.5 High-energy Channel of COSI's ACS

The high-energy channel of the ACS, ranging from 2 to 40 MeV electron equivalent (MeVee), is crucial to obtain information about highly energetic particles, approximating the radiation damage to GeDs, and modeling the high-energy background. We performed measurements for a crude calibration of COSI's ACS high-energy channel at the UC Davis Proton Beam test facility with an original beam energy of 64 MeV. The spectra shown in Fig. 7 reflect the performance of the high-energy channel.

3. Conclusions

The Anti-Coincidence Subsystem on the Compton Spectrometer and Imager is crucial to many science goals and to the reduction of background in the GeD data. With the improvements made through the development process outlined in this paper, we are able to run the ACS system with

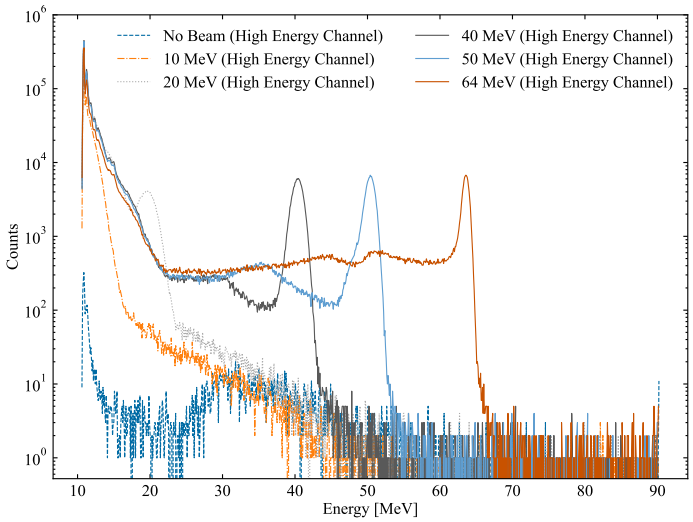

Figure 7: Calibrated energy spectra from the high-energy (proton) channel of one BGO detector in the ACS. Shown is an original 64 MeV proton beam and other attenuated energies, 50 MeV, 40 MeV, 20 MeV, 10 MeV.

a very low energy threshold and obtain good energy resolution. This low energy threshold is critical in vetoing of incomplete events in the GeD and therefore improving the sensitivity of the GeD instrument. The low energy threshold is also crucial for detection of GRBs, which emit predominately at lower energies. The research also helps us save power which leaves a high margin for other high-power consuming parts on the spacecraft.

References

[1] I. Johnson, W. N. and R.C. Haymes, *ApJ* **184** (1973) 103.

[2] R. Diehl, *arXiv preprint arXiv:1307.4198* (2013) .

[3] A.W. Lowell, S.E. Boggs, C. Chiu, C.A. Kierans, C. Sleator, J.A. Tomsick et al., *The Astrophysical Journal* **848** (2017) 119.

[4] A. Zoglauer, T. Siegert, A. Lowell, B. Mochizuki, C. Kierans, C. Sleator et al., *arXiv preprint arXiv:2102.13158* (2021) .

[5] J. Tomsick, S. Boggs, A. Zoglauer, D.H. Hartmann, M. Ajello, E. Burns et al. in *38th International Cosmic Ray Conference*, p. 745, Sept., 2024, DOI [2308.12362].

[6] C.C. Sleator, E.A. Wulf, A. Lowell, B. Mochizuki, A. Joens, G. de Geronimo et al. in *2023 IEEE Nuclear Science Symposium, Medical Imaging Conference and International Symposium on Room-Temperature Semiconductor Detectors (NSS MIC RTSD)*, pp. 1–2, 2023, DOI.

[7] R. Mao, L. Zhang and R.-Y. Zhu in *2007 IEEE Nuclear Science Symposium Conference Record*, vol. 3, pp. 2285–2291, IEEE, 2007.

[8] L. Nava, G. Ghirlanda, G. Ghisellini and A. Celotti, *Astronomy & Astrophysics* **530** (2011) A21.

[9] J.E. Grove and W.N. Johnson in *Space Telescopes and Instrumentation 2010: Ultraviolet to Gamma Ray*, vol. 7732, pp. 138–148, SPIE, 2010.